

# First principles simulations of liquid Fe-S under Earth's core conditions

Dario Alfè and Michael J. Gillan

*Physics Department, Keele University, Keele, Staffordshire ST5 5BG, U.K.*

(September 30, 2018)

## Abstract

First principles electronic structure calculations, based upon density functional theory within the generalized gradient approximation and ultra-soft Vanderbilt pseudopotentials, have been used to simulate a liquid alloy of iron and sulfur at Earth's core conditions. We have used a sulfur concentration of  $\approx 12\%$ wt, in line with the maximum recent estimates of the sulfur abundance in the Earth's outer core. The analysis of the structural, dynamical and electronic structure properties has been used to report on the effect of the sulfur impurities on the behavior of the liquid. Although pure sulfur is known to form chains in the liquid phase, we have not found any tendency towards polymerization in our liquid simulation. Rather, a net S-S repulsion is evident, and we propose an explanation for this effect in terms of the electronic structure. The inspection of the dynamical properties of the system suggests that the sulfur impurities have a negligible effect on the viscosity of Earth's liquid core.

PACS numbers: 61.25.Mv, 66.20.+d, 66.30.Jt, 71.15.Pd

arXiv:cond-mat/9804035v1 3 Apr 1998

## I. INTRODUCTION

The Earth's liquid outer core consists mainly of molten iron, but its density is about 10% too low to be pure iron [1], so it must contain also some light element. The nature of the light element is still uncertain, and during the last forty-five years the main proposed candidates have been carbon [1–3], silicon [1,4–7], magnesium [8], sulfur [2,3,9–12], oxygen [8,9,13] or hydrogen [1,14,15]. Due to motivations based on cosmic abundance, models of Earth formation, and ability to dissolve into liquid iron [16–18], sulfur seems to be one of the most likely light elements in the core. The properties of liquid iron and iron alloys under very high pressures are of fundamental importance in understanding the dynamics of the Earth's core, but they are difficult to investigate because of the extreme conditions involved. A particularly important property is the viscosity of the outer core, since it determines the convective internal motions which are responsible for the generation of the Earth's magnetic field.

First principles calculations have been shown to be very reliable for the prediction of the structural and dynamical properties of a variety of materials, including liquid metals [19–21]. Since selenium and sulfur have very similar properties, it is relevant to mention previous *ab initio* calculations of the structural, dynamical, and electronic properties of liquid Ag-Se alloys [22] and liquid Se [23], which have been shown to be in very good agreement with experiments. Our own *ab initio* calculations on pure liquid iron under Earth's core conditions have demonstrated that the structure of the liquid is close packed, with a coordination number  $\geq 12$  and a diffusion coefficient of the same order of magnitude as those of many liquid metals at ambient pressure [24,25].

We report here on a first principles investigation of the structural, dynamical, and electronic structure properties of a liquid alloy of iron and sulfur under Earth's core condition. We have simulated a liquid alloy with a 12% wt sulfur concentration, in line with the maximum estimates for the sulfur abundance in the core [26].

To our knowledge the only high pressure experimental work on a liquid iron sulfur alloy is that of LeBlanc and Secco [27]. They have studied a  $\text{Fe}_{73}\text{S}_{27}$  (wt%) (with the notation of the original reference) liquid in a range of pressures between 2 and 5 GPa and temperatures between 1100 and 1300°C, and found a value for the viscosity about three order of magnitude higher than the ambient pressure value. They have tentatively attributed this high viscosity value to the formation of sulfur chains, or clusters. These aggregates would impede the diffusion of the atoms in the liquid, resulting in an enhancement of the viscosity. Whether or not a similar sulfur effect could be present also in the Earth's liquid core is a matter of current dispute. We remark that the temperatures studied by LeBlanc and Secco are much lower and their pressures very much lower than those in the Earth's core, so that it is not obvious that their results have any relevance to the properties of the core.

The paper is organized as follows. In section II we discuss the theoretical framework, and in section III we present our results for some solid Fe-S crystal structures, compared with other theoretical work. Then, in section IV we pass to the discussion of the liquid, focusing our attention on the structural (IV A), electronic (IV B), and dynamical properties (IV C). Finally we present our conclusions.

## II. METHOD

The first principles calculations presented here are based on density functional theory within the generalized gradient approximation (GGA) [28]. The electronic wave-functions are expanded in a plane-wave basis set with a cut-off energy of 350 eV, and the electron-ion interaction is described by means of ultrasoft Vanderbilt pseudopotentials (PP) [29], which allow one to use a much lower number of plane-waves, comparing with a standard norm-conserving PP, without affecting the accuracy of the calculations. In the PP approximation only the valence electrons are taken into account, while the tightly bound core electrons are excluded from the calculation. This approximation is usually perfectly justified, and has been demonstrated to reproduce very well the all electron results for transition metals. In particular, it has been accurately checked for iron in our previous work [24,25]. In spite of this strong evidence, we considered it worthwhile to do some calculations of the structural properties of solid FeS, and compare them with all-electron full potential calculations of the same properties. The results of these calculations are reported in the next section.

The iron PP is the same as that used in Refs. [24,25], and has been constructed with a frozen [Ar] core and a  $4s^1 3d^7$  reference valence configuration. The sulfur PP was constructed with the [Ne] core and the  $3s^2 3p^4$  reference configuration for the valence states. At the pressure conditions of the Earth's core the distance among the atoms may become so small that the ionic cores overlap. This may result in a degradation of the PP approximation. The iron PP has been constructed so as to minimize this problem, and its quality has been checked elsewhere [24,25]. The reliability of the sulfur PP will be assessed in the next section. Non-linear core corrections [30] are included throughout this work.

The simulation of the liquid has been performed using *ab initio* molecular dynamics (AIMD), with the forces calculated fully quantum mechanically (within the GGA and the PP approximations), and the ions moved according to the classical equation of motion. We have used a supercell approach with periodic boundary conditions. The first pioneering work in AIMD was that of Car and Parrinello (CP) [31], who proposed a unified scheme to calculate *ab initio* forces on the ions and keep the electrons close to the Born-Oppenheimer surface while the atoms move. We have used here an alternative approach, in which dynamics is performed by explicitly minimizing the electronic free energy functional at each time step. This minimization is more expensive than a single CP step, but the cost of the step is compensated by the possibility of making longer time steps. The molecular dynamics simulations presented here have been performed using VASP (Vienna *ab initio* simulation package). In VASP the electronic ground state is calculated exactly (within a self-consistent threshold) at each MD step, using an efficient iterative matrix diagonalization scheme and a Pulay mixer [32]. Since we are interested in finite temperature simulations, the electronic levels are occupied according to the Fermi statistics corresponding to the temperature of the simulation. This prescription also avoids problems with level crossing during the self-consistent cycles. For more details of the VASP code see Refs. [33,34].

Within this approach to AIMD it is important to provide a good starting electronic charge density at each time step, so as to reduce the number of iterations to achieve self-consistency. This is done usually by a quadratic (or even multilinear) extrapolation of the charge. We have used here a different scheme: at the beginning of each time step the electronic charge density is extrapolated using the atomic charge density and a quadratic

extrapolation on the difference, i.e. the charge is written as:

$$\rho(t) = \rho_{at}(t) + \delta\rho(t), \quad (1)$$

where  $\rho(t)$  is the self-consistent charge density at time  $t$ , and  $\rho_{at}(t)$  is the sum of the atomic charges. At time  $t + dt$  the charge is written as the sum of the atomic charges, which can be calculated exactly and cheaply, and a quadratic extrapolation on  $\delta\rho$ . We have found that for liquid iron this scheme provides a much better starting charge compared with a conventional extrapolation of the whole charge, resulting in a reduction of CPU time of almost a factor two.

### III. SOLID FES

Solid FeS adopts a modified NiAs structure at zero pressure [35], and undergoes a first phase transition into a MnP structure at 3.4 GPa [36] and a second transition into an unknown structure at 6.7 GPa [37–39]. Mao *et al.* have found FeS in an orthorhombic distorted B1 structure at pressure above 11.5 GPa [40]. Sherman [41] has done theoretical spin-unrestricted calculations on three possible crystal structures. He has used the full potential linearized augmented plane wave method (FLAPW) to study FeS in the NiAs(B8), CsCl(B2), and NaCl(B1) crystal structures. He found that the CsCl structure is the most stable at high pressure.

To confirm the accuracy of the pseudopotential approximation, we have repeated the same calculations. For each structure energy convergence with respect to  $\mathbf{k}$ -points sampling has been checked. We have found total energies to be converged within 10 meV per atom by using 30, 20 and 10  $\mathbf{k}$ -points in the irreducible Brillouin zone of the FeS(B8), FeS(B2) and FeS(B1) structures respectively. In the FLAPW calculations the non-magnetic phase for the three sulfides was found to be more stable than the magnetic one. We have found instead that the magnetic phase is more stable for the B2 and the B8 compounds (we have actually found that the B8 phase is anti-ferromagnetic), while only the B1 phase shows no magnetic moment at all the volumes investigated. In Fig. 1 we display the total energy as a function of the volume for the B2 and the B8 structures compared with the same calculations done in a spin-restricted scheme. The difference in the total energy is clearly evident at low pressures. However, this becomes negligibly small (even if never zero for the B2 structure) at high pressure. We want to point out that the disagreement regarding the magnetism between our calculations and FLAPW calculations is unlikely to be due to the PP approximation, as also previous calculations on the structure of solid pure iron have shown to be in very good agreement with all-electron calculations [24,25]. In Fig. 2 we display spin-unrestricted PP and FLAPW data, and in Tab. I we report the equilibrium density  $\rho_0$ , the bulk modulus  $K$ , and its derivative with respect to pressure  $K'$ , as obtained from a fit of the data to a Birch-Murnaghan equation of state, both for a spin-restricted and a spin-unrestricted calculation. The FLAPW data for the B8 and the B1 structures are not reported in Ref. [41] and have been deduced from a fit of the data to a Birch-Murnaghan equation of state. Our calculated transition pressure from the B8 to the B2 structure is 97 GPa, to be compared with 75 GPa obtained in the FLAPW calculations. Since the FLAPW results are non-magnetic, the non-magnetic PP calculations have to be compared

with them. Despite the slight difference in the equilibrium density, the agreement between our non-magnetic calculations and FLAPW data is good, and confirm the reliability of our PP calculations.

In order to check any possible effects at high pressure due to core overlaps, we have repeated the calculations using a different sulfur PP constructed with a shorter core radius (1.8 a.u. instead of 2.2 a.u.). We have not found any appreciable difference between the two, and we have decided to use the PP having the large core radius for the simulation of the liquid.

#### IV. THE LIQUID

The possible amount of sulfur in the Earth's core is not certain, and recent estimates provide a range from a few % wt to a maximum of  $\approx 10\%$  wt [26]. Since the effect of sulfur is likely to be larger for larger concentrations, we decided to use the highest possible amount of sulfur compatible with the current estimates. In our simulations we have used 64 atoms in a cubic supercell. The numbers of iron and sulfur atoms were 52 and 12 respectively, resulting in  $\approx 12\%$  wt concentration and molar fraction of  $x_{Fe} = 0.8125$  and  $x_S = 0.1875$ . In the liquid structure the system is close packed. Since the majority of atoms are irons and since in the hexagonal close packed structure solid iron is non-magnetic at high pressure [42], we have used spin-restricted calculations for all the liquid simulations. A spin-unrestricted calculation on one configuration of the liquid has confirmed that this is actually non-magnetic.

One of the possible effects of the impurities is the formation of linear chains or small clusters. This fact could have important effects on the transport properties of the whole liquid alloy, since the impurity chains would impede the diffusion of the atoms, and therefore would increase the viscosity. In order to address this possible effect, we decided to carry out two independent simulations, starting with two very different atomic distribution configurations. In the first case we have taken a previous pure liquid iron simulation [24] and substituted randomly iron with sulfur; we will refer to this simulation as RS. In the second case we have explicitly created a sulfur cluster, by transforming a chosen iron atom together with 11 of its nearest neighbors into sulfur atoms; we refer to this simulation as CS. The CS case has been performed to give the sulfur atoms all the possible chances to stay together.

Both the simulations have been done at a thermodynamic point representative of the boundary between the Earth's solid inner core and the liquid core. Here the temperature  $T$  is uncertain; estimates range from 4000 to 8000 K [43]. The pressure is accurately known, and it is 330 GPa [43]. In order to compare the results of the present work with those obtained for pure iron [24,25] we have used the same temperature  $T = 6000$  K. Since the sulfur has approximately the same size as iron at this pressure, we argue that a small quantity of sulfur should not change appreciably the pressure and therefore we have also used the same volume per atom as in Refs. [24,25]. This resulted in a  $\approx 8\%$  lower density, i.e.  $\rho = 12.33$  g/cm<sup>3</sup> (for pure iron it was  $\rho = 13.30$  g/cm<sup>3</sup>). The Brillouin zone sampling has been restricted to the  $\Gamma$  point only, and the integration of the classical equation of motion has been done using the Verlet algorithm [44]. The temperature was controlled using a Nosé thermostat [45,46]. The quality of the simulation has been checked by looking at the constant of motion; this usually shows a drift which is due to a bad integration of the equation of

motion (time step too large) and/or a bad calculation of the forces. These effects can both be easily controlled by acting on the time step and on the self-consistency threshold on the electronic minimization, which determines the accuracy with which the forces are computed. However, a too short time step and/or a too small self-consistency threshold may require a too expensive computational effort, so one has to choose a judicious compromise. We have used a self-consistency threshold on the total energy of  $1.5 \times 10^{-7}$  eV/atom and a time step of 1 fs; with these prescriptions the drift of the constant of motion has been kept less than  $\approx 7 - 8$  meV/atom per ps. We have simulated the RS system for 10 ps and the CS one for 3 ps. These simulations are continuations of a previous pure iron simulation [24,25], and then our starting configuration would be an equilibrium configuration if we had only iron. Since we suddenly transformed some iron atoms into sulfur atoms, this is not in principle an equilibrium configuration for the new system. The time needed to go from the equilibrium configuration of pure liquid iron to that of the alloy is also an interesting quantity. For this reason no equilibration time has been considered, and we report the whole simulations starting from the very beginning.

### A. Structure

The structural properties of the system have been inspected by looking at the partial radial distribution functions (rdf),  $g_{FeFe}(r)$ ,  $g_{FeS}(r)$ , and  $g_{SS}(r)$ . The partial rdf's are defined in such a way that, sitting on one atom of the species  $\alpha$ , the probability of finding one atom of the species  $\beta$  in the spherical shell  $(r, r+dr)$  is  $\rho_\beta 4\pi r^2 g_{\alpha\beta}(r) dr$ , where  $\rho_\beta = x_\beta/V$  is the number density of the species  $\beta$  and  $V$  is the volume per atom.

In Fig. 3 we display the rdf's calculated from 2.5 ps time averages taken at four different starting times for the RS simulation. The four pictures provide a time analysis of the liquid structure. The two  $g_{FeFe}(r)$  and  $g_{FeS}(r)$  remain essentially unchanged throughout the simulation. Liquid sulfur is known to form chains [47], the distance among the atoms for each pair being  $\approx 2$  Å at zero pressure. If sulfur formed chains also in the present case, this would result in a peak in the  $g_{SS}(r)$  at the position of the bond length. If sulfur just behaved as though it was iron, then its partial rdf would be identical to the iron one. We have not found either of the two behaviors. The form of the  $g_{SS}(r)$  clearly indicates that sulfur behavior is different from iron, and at the same time it is also evident that sulfur atoms do not form chains. Rather, a S-S repulsion is suggested. The same indications come also from an inspection of the partial structure factors (not reported). The analysis of the CS simulation is even more interesting. In Fig. 4 we display the rdf's for the second simulation. In this case in the first panel of the figure we display the rdf's averaged only over the first 0.5 ps of the simulation. The reason for this short average time is that we have found that the sulfur cluster dissociates quickly, and only in this very short time can its existence be monitored. This is evident from the presence of a peak in the  $g_{SS}$  at  $\approx 2$  Å. In the second panel of the figure we display the partial rdf's averaged over the last 2 ps of the simulation, i.e. starting the average 1 ps after the beginning of the simulation. It is evident that the cluster has completely dissociated and the rdf's have become essentially identical to those of the RS simulation. It is also interesting to compare the structural properties of the alloy with those of the pure liquid iron. In Fig. 5 we display the iron rdf as calculated in Ref. [24] and the  $g_{FeFe}$  calculated here. The two are very similar, and provide evidence that a small

percentage of sulfur impurity does not appreciably affect the properties of the liquid.

The integration of the first peak of the rdf's provides a definition of the coordination number  $N_{\alpha\beta}^c$ :

$$N_{\alpha\beta}^c = \rho_\beta \int_0^{r_{\alpha\beta}^c} 4\pi r^2 g_{\alpha\beta}(r) dr, \quad (2)$$

where  $r_{\alpha\beta}^c$  is the position of the minimum after the first peak of  $g_{\alpha\beta}$ . In pure iron liquid it was found  $N_{FeFe}^c = 13.8$  [24]. In the present case we find  $N_{FeFe}^c = 11.2$  (which is essentially  $13.8 \times x_{Fe}$ , since the two  $g_{FeFe}$ 's are practically equal). The integration of  $g_{FeS}$  provides coordination numbers  $N_{FeS}^c = 2.5$  and  $N_{SFe}^c = 10.8$ , i.e. each iron atom is surrounded by 2.5 sulfur atoms, and each sulfur atom by 10.8 iron atoms. We will comment in the Discussion section on these numbers.

Two main conclusions can be drawn from these results. The first is that the system equilibrates quickly: in the RS case there is no evidence of equilibration time at all, and this means that the equilibrium configurations of the liquid alloy, when this is built up distributing impurity atoms in a random way throughout the liquid, are not much different from those of the pure liquid; the starting configuration of the CS case has been constructed so that there is an explicit separation of sulfur from iron, and in this case the system is not in an equilibrium configuration, but the equilibration time is very short (of the order of 1 ps), and after that time the random distribution of the impurities throughout the liquid is restored. The second conclusion is more important: there is no evidence of sulfur clustering or formation of linear chains; rather, a sulfur-sulfur repulsive tendency is apparent. We will try to explain this effect in the discussion of the electronic properties of the system in the next section.

## B. Electronic structure

The structural behavior of the system can be understood in terms of the electronic structure. In particular, the interesting quantities are the relative strengths of the Fe-Fe, Fe-S, and S-S bonds. In Fig. 6 we display the electronic density of states (DOS), i.e. the total number of electronic states per unit energy, for the configuration of the RS simulation corresponding at  $t = 7.9$  ps. Having in mind a tight binding interpretation of the chemical bonds among the atoms, it is particularly useful to inspect the local density of states (LDOS), i.e. the DOS for each atomic species decomposed into angular momentum resolved contributions. The  $(l, m)$  angular momentum component of the atom  $i$  is the projection onto the spherical harmonic  $(l, m)$  of all the wavefunctions in a sphere of radius  $R$  centered on the atom  $i$ . For more details about how the projections are done see Ref. [51]. The LDOS averaged over all the atoms of each species in the cell is also displayed in Fig. 6. The value of the sphere radius  $R$  is somewhat arbitrary. We have used  $R = 0.8 \text{ \AA}$  for both iron and sulfur, which is roughly half the minimum distance between the atoms, and thus should not attribute to one atom possible contributions to the LDOS deriving from neighboring atoms.

Many features are evident in the DOS; referring all the energies to the Fermi energy, there is a small peak at  $\approx -18$  eV, a shoulder at  $\approx -10$  eV, a main broad peak extending from  $\approx -10$  eV to  $\approx 5$  eV and a broad feature well above the Fermi energy. These features can be easily related to the LDOS shown in the lower panel of Fig. 6. The peak at  $\approx -18$

eV is the S(3s) level, which is isolated from the rest of the DOS. The shoulder at  $\approx -10$  eV is mainly due to S(3p), even if a small Fe(3d) contribution is also present. The main peak extending from  $\approx -10$  eV to  $\approx 5$  eV is essentially Fe(3d) and the feature at  $\approx 8$  eV is due to S(3d) and Fe(3d). The Fe(4s) and Fe(4p) orbitals are not reported; they are small contributions to the DOS extending from  $\approx -10$  eV to  $\approx 15$  eV. Disregarding the S(3s) level, we can focus our attention on the S(3p), S(3d) and Fe(3d) bands. The S(3p) band shows a main peak at  $\approx -10$  eV and a somewhat less intense peak above the Fermi energy, at  $\approx 3$  eV; the Fe(3d) band has a small shoulder at the same position as the main S(3p) peak and extends well above the Fermi energy. Since the LDOS depend on the choice of the sphere radius  $R$ , we have repeated the same analysis using a smaller radius,  $R = 0.6$  Å. Because of the reduced sphere radius, the absolute intensity of the peaks is also reduced. This is more true for the sulfur bands, which are less localized around the nuclei than the iron 3d band. However, the relative intensity of the S(3p) peaks at  $-10$  and  $3$  eV is essentially the same as that for  $R = 0.8$  Å. This fact demonstrates that these two peaks are bonding and anti-bonding states. We will demonstrate later that they actually result from a S(3p)-Fe(3d) hybridization. Assuming for the moment that this is the case, we can state that the sulfur-iron bond is predominantly covalent. A careful inspection of the LDOS reveals that part of the sulfur-iron bond is also due to S(3d)-Fe(3d) hybridization. The bonding between Fe atoms occurs by the well known mechanism of partial filling of the 3d-band (this is the mechanism emphasized by Friedel's analysis [48] of the cohesive and elastic properties of transition-metal crystals). The splitting of the sulfur-iron bonding and anti-bonding levels is a measure of the strength of the bonds. Since this is larger than the broadening of the Fe(3d) band we argue that the Fe-S bond is stronger than the Fe-Fe one. This is consistent with the different forms of the rdf's described in the previous section, where it was evident that the average Fe-S distance is lower than the Fe-Fe one.

In order to disentangle the S-S neighboring effect from the S-Fe one, we have used the RS simulation to analyze the LDOS of two sulfur atoms in two different environments. The first one, S<sub>1</sub>, has been chosen so as to maximize the number of sulfur atoms in the nearest neighbors shell, and it has 2 sulfur atoms and 9 iron atoms at a distance less than 2.5 Å; while the second atom, S<sub>2</sub> has been chosen so that there are no sulfur atoms within the nearest neighbors shell. In this way S<sub>1</sub> makes bonds with other sulfur atoms, while S<sub>2</sub> bonds only with iron atoms. In the upper panel of Fig. 7 we display the LDOS of S<sub>1</sub> and S<sub>2</sub> for the 3s and the 3p bands. For the S<sub>2</sub> atom (no sulfur bonds) a sharpening of both the 3s and the 3p peaks can be observed, when compared with the averaged LDOS. This demonstrates that the bonding and the anti-bonding peaks do not result from a S-S bond, and they are actually due to S-Fe hybridization. The analysis of the projections onto the S<sub>1</sub> atom allows us to infer about the strength of the S-S bonds. In this case S<sub>1</sub> is close to other two sulfur atoms, and the effect of the S-S orbital overlaps is evident: there is a nice splitting of the 3s level and a splitting-broadening of the 3p level. Since both the 3s and the 3p peaks are far from the Fermi energy, there is no appreciable energy gain when two sulfur atoms come close. This means that the two different environments (some sulfur in the first neighbor shell and no sulfur in the first neighbor shell) are energetically almost equivalent, so that there is no sulfur-sulfur bond at all.

It is interesting to notice that the 3s splitting is larger than the 3p splitting. This is not what one would expect for a couple of isolated sulfur atoms, since the 3s orbitals are more



localized than the  $3p$  orbitals in the free atom, and therefore they would overlap less. But in the present case this behavior is perfectly consistent and it is a further demonstration of the sulfur-iron bonding strength. The  $3p$  orbitals are hybridized with the surrounding iron atoms, while the  $3s$  orbitals are well localized on the sulfur atoms, since they essentially do not interact with iron. Because of this different spatial distribution, when two sulfur atoms come together the  $3s$  orbitals overlap more effectively than the  $3p$  ones, which are engaged with iron, and this results in the larger splitting observed in Fig. 7.

A further evidence of the Fe-Fe and Fe-S bond strength difference can be inferred by the inspection of the effect of the sulfur neighborhood on the iron atoms. In the lower panel of Fig. 7 we display the Fe( $3d$ ) band for two selected iron atoms. The first, Fe<sub>1</sub> has 6 Fe and 4 S within a distance of 2.5 Å, while the second, Fe<sub>2</sub>, has 11 Fe and 1 S within the same distance. A comparison of the two bands clearly shows that Fe<sub>1</sub>, the iron atom with more sulfur nearest neighbors, has a broader  $3d$  band with respect to Fe<sub>2</sub>. Since the band extends across the Fermi level, a broader band results in a lowering of the energy, and then the Fe-S bond must be stronger than the Fe-Fe one. The strength difference of the two Fe-Fe and Fe-S bonds is expected from the relative extension of the sulfur  $3p$ ,  $3d$  and the iron  $3d$  orbitals: since the sulfur orbitals are less localized around the nuclei than the iron ones, they overlap with iron more effectively, leading to a larger broadening of the Fe( $3d$ ) band.

In conclusion, the sulfur-sulfur repulsion evident from the analysis of the structural properties is not a real repulsion effect, but it is rather due to the stronger iron-sulfur interaction with respect to the iron-iron and the sulfur-sulfur ones. The iron atoms want to be as much coordinated as possible with sulfur atoms, while the sulfur-sulfur interaction is negligible. The combination of these two facts produces highly sulfur coordinated iron atoms (compatibly with the concentration) and isolated sulfur atoms. The consequences for the transport properties of the liquid will be discussed in the next section.

### C. Dynamics

In the liquid phase the atoms are free to diffuse throughout the whole volume, and this behavior can be characterized by diffusion coefficients  $D_\alpha$  for the two species of atoms, which are straightforwardly related to the mean square displacement of the atoms through the Einstein relation [49]:

$$\frac{1}{N_\alpha} \left\langle \sum_{i=1}^{N_\alpha} |\mathbf{r}_{\alpha i}(t_0 + t) - \mathbf{r}_{\alpha i}(t_0)|^2 \right\rangle \rightarrow 6D_\alpha t, \quad \text{as } t \rightarrow \infty, \quad (3)$$

where  $\mathbf{r}_{i\alpha}(t)$  is the vector position at time  $t$  of the  $i$ -th atom of species  $\alpha$ ,  $N_\alpha$  is the number of atoms of species  $\alpha$  in the cell, and  $\langle \rangle$  means time average over  $t_0$ . In studying the long time behavior of the mean square displacement, it is convenient to define a time dependent diffusion coefficient  $D_\alpha(t)$ :

$$D_\alpha(t) = \frac{1}{6tN_\alpha} \left\langle \sum_{i=1}^{N_\alpha} |\mathbf{r}_{\alpha i}(t_0 + t) - \mathbf{r}_{\alpha i}(t_0)|^2 \right\rangle, \quad (4)$$

which has the property that

$$\lim_{t \rightarrow \infty} D_\alpha(t) = D_\alpha. \quad (5)$$

In Fig. 8 we display the iron and the sulfur diffusion coefficients calculated using Eq. (4) for the RS simulation. The four different panels refer to four different time windows, each of length 2.0 ps, and starting respectively at  $t_{window}$  equal 0, 2.0, 4.0 and 6.0 ps from the beginning of the simulation. That is, for each window  $D_\alpha(t)$  is averaged from  $t_0 = t_{window}$  to  $t_0 = t_{window} + 2.0$ . We recall again that no equilibration time has been excluded, so that possible non-equilibrium effects should be evident from systematic different results in the succession of the time windows. The meaningful quantity that has to be extracted from the pictures is the limit of  $D_\alpha(t)$  for large times. Once again, there is no evidence of time dependent behavior, and the diffusivity is approximately the same in all the windows. The difference that can be appreciated from the different windows is an estimate of the statistical error on  $D_{Fe}$  and  $D_S$ . From this data we can estimate  $D_{Fe} \approx 0.4 - 0.6 \times 10^{-4} \text{ cm}^2 \text{ s}^{-1}$  and  $D_S \approx 0.4 - 0.6 \times 10^{-4} \text{ cm}^2 \text{ s}^{-1}$ , which are very similar. The value of the iron diffusion coefficient is very close to that found by Vočadlo *et al.* [24] for pure iron at the same temperature and  $\rho = 13.3 \text{ g/cm}^3$ , which was  $D_{Fe} \approx 0.4 - 0.5 \times 10^{-4} \text{ cm}^2 \text{ s}^{-1}$ .

The viscosity of the liquid could in principle also be directly calculated from the AIMD simulation, *via* the autocorrelation function of the off-diagonal part of the stress tensor [50]. But this would be a major undertaking, and in fact the viscosity has not yet been calculated for any system by AIMD. The reason is that, by contrast with the diffusion coefficient, only the average over time origins can be done in this case, so that the statistics is worse by a factor  $N_{at}$  then that of the diffusion coefficient. This implies that for a meaningful measure of the viscosity a much longer run would be needed. An alternative way to obtain a rough estimate of the viscosity is by using its relationship with the diffusion coefficient stated by the Stokes-Einstein relation:

$$D\eta = \frac{k_B T}{2\pi a}, \quad (6)$$

as was done in our recent calculation on pure liquid iron [24,25]. This relation is exact for the Brownian motion of a macroscopic particle of diameter  $a$  in a liquid of viscosity  $\eta$ . The relation is only approximate when applied to atoms; however, if  $a$  is chosen to be the nearest neighbors distance of the atoms in the solid, Eq. (6) provide results which agree within 40% for a wide range of liquid metals.

In the present case we have two atomic species, each of them with its own diffusion coefficient. However, iron and sulfur have a similar atomic radius at this high pressure, and the similar values for the two diffusion coefficients that we have found are consistent with the form of the Stokes-Einstein relation, and provide also an indirect check of its applicability in this particular case. Since the pure iron diffusion coefficient [24,25] is essentially equal to that found with the present amount of sulfur impurity, we conclude that the latter has very little effect on the viscosity of the Earth's liquid outer core. This means that the value of  $\eta \approx 1.3 \times 10^{-2} \text{ Pa s}$  obtained in our simulation on pure liquid Fe [24,25] should also be valid for the present Fe-S mixture.

## V. DISCUSSION AND CONCLUSIONS

We have used first principles calculations based on density functional theory within GGA for the exchange-correlation energy and ultrasoft pseudopotentials to simulate a liquid iron-sulfur alloy at Earth's core conditions ( $T = 6000$  K,  $\rho = 12.33$  g/cm<sup>3</sup>, and a molar fraction of S = 0.1875). We have found that all atoms are closed packed, so that the total number of neighbors surrounding each atom is  $\geq 12$ . As far as Fe-Fe and Fe-S correlations are concerned, the distribution of Fe and S atoms is essentially random. But S-S correlation shows an effective repulsion between S atoms, so that the probability of finding an S atom in the nearest neighbors shell of a given S atom is much less than would be obtained with a random distribution. We have presented strong evidence to show that there is no tendency whatever for S atoms to form chains.

Our study of the electronic structure shows that the bonding is predominantly metallic/covalent. Our calculated electronic density of states demonstrates that S form occupied bonding and unoccupied anti-bonding states with neighboring Fe atoms. The resulting covalent S-Fe bond is considerably stronger than the bond between Fe atoms, as we have seen from the magnitude of the energy splitting between the bonding and the anti-bonding states. We have argued that the strength of this bond comes from the large spatial overlap between the S(3*p*) and Fe(3*d*) states. By contrast, sulfur atoms do not make bonds between each other. The strength of the S-Fe bond compared with the other two explains the effective repulsion behavior between S atoms: if two S atoms come together two Fe-S bonds are lost and one Fe-Fe bond is formed, and the total energy is increased.

Now we come back to the question of the Fe-Fe, Fe-S, and S-S coordination numbers. If sulfur and iron were equal, and their distributions random, one would expect  $N_{FeS}^c = 13.8 \times x_S \approx 2.6$  and  $N_{SFe}^c = N_{FeFe}^c = 11.2$ . Since the Fe-S bond is stronger than the other two, this should result in higher Fe-S and S-Fe coordination numbers. On the contrary, we find two slightly smaller values,  $N_{FeS}^c = 2.5$  and  $N_{SFe}^c = N_{FeFe}^c = 10.8$ . However, since iron and sulfur stay closer than iron and iron (as can be checked by the inspection of the rdf's), the space left to iron atoms to surround the sulfur is reduced, and therefore the coordination number is correspondingly lowered.

Our analysis of the dynamics of the Fe and S atoms shows that the liquid alloy has essentially the same transport properties as the pure iron liquid. We have calculated iron and sulfur diffusion coefficients which are both of  $\approx 0.4 - 0.6 \times 10^{-4}$  cm<sup>2</sup> s<sup>-1</sup>, very similar to that of pure liquid iron,  $\approx 0.4 - 0.5 \times 10^{-4}$  cm<sup>2</sup> s<sup>-1</sup>, as calculated in Ref. [24]. This also means that the iron-sulfur bonds in the liquid, although stronger than iron-iron bonds, are not strong enough to form molecules or polymers, at least at these conditions of pressure and temperature. Since the diffusion coefficients can be related to the viscosity of the liquid *via* the Stokes-Einstein relation, we conclude that the sulfur impurity has small effects, if any, on the viscosity of the Earth's liquid core.

The results discussed in this paper seem at first sight rather difficult to reconcile with the experimental work of LeBlanc and Secco [27], who found for a Fe-S mixture an anomalous increasing of the viscosity with pressure. However, we must point out that the conditions studied were quite different, so that it is not obvious that the two works could be compared. We suggest that a future first principles investigation for a system with the same conditions of concentration, pressure and temperature as those of that experimental work could be

interesting.

Finally, we think that a direct first principles calculation of the viscosity *via* the auto-correlation function of the off-diagonal term of the stress tensor is not completely out of the question, and we are thinking now to address some effort in this direction.

## VI. ACKNOWLEDGMENTS

The work of DA is supported by NERC grant GST/O2/1454. We thank the High Performance Computing Initiative for allocations of time on the Cray T3D and T3E at Edinburgh Parallel Computer Centre, these allocations being provided through the Minerals Consortium and the U.K. Car-Parrinello Consortium. We thank Dr. G. Kresse and Dr. G. de Wijs for valuable technical assistance, and Dr. D. Sherman for useful discussions.

## TABLES

TABLE I. Structural parameters for three different FeS crystal structures calculated using a fit to a Birch-Murnaghan equation of state.  $\rho_0$  is the equilibrium density,  $K$  the bulk modulus and  $K'$  its derivative with respect to pressure. In the first column we report FLAPW data [41]. In the second and in the third columns we report our calculations in a spin-restricted and spin-unrestricted PP formalism.

		FLAPW	PP(spin-unrestricted)	PP(spin-restricted)
CsCl	$\rho_0(\text{g/cm}^3)$	6.18	6.0	6.35
	$K(\text{GPa})$	190	143	191
	$K'$	4.06	4.09	4.11
NiAs	$\rho_0(\text{g/cm}^3)$	5.67	5.55	5.94
	$K(\text{GPa})$	178	114	176
	$K'$	4.31	4.84	4.34
NaCl	$\rho_0(\text{g/cm}^3)$	5.58	5.77	5.77
	$K(\text{GPa})$	171	176	176
	$K'$	3.87	3.95	3.95

## FIGURES

FIG. 1. Comparison between PP spin-restricted and spin-unrestricted calculations of the energy as a function of the volume for FeS in the CsCl (B2) and in the NiAs (B8) structures.

FIG. 2. Spin-unrestricted calculated energy-volume curves for FeS in the NiAs(B8) and CsCl(B2) structures. The curves are obtained from a fit of the data to a Birch-Murnaghan equation of state. FLAPW calculations [41] are reported for comparison.

FIG. 3. Radial distribution functions calculated by averaging over four successive time windows in the simulation starting with S atoms in random positions.

FIG. 4. Radial distribution functions calculated by averaging over the first 0.5 ps (left panel), and over 2 ps after 1 ps of equilibration (right panel) for the simulation started with the sulfur atoms near each other (CS simulation, see text).

FIG. 5. Iron-iron radial distribution functions calculated in the pure liquid simulation [24] and in the present liquid alloy simulation.

FIG. 6. Total electronic density of states (upper panel) and density of states for each atomic species decomposed into angular momentum contributions (lower panel).

FIG. 7. LDOS for two selected sulfur atoms (upper panel) and two selected iron atoms (lower panel). The atoms  $S_1$  and  $S_2$  have respectively 2 and 0 sulfur atoms at distance less than 2.5 Å, and 9 and 11 iron atoms within the same distance. The atoms  $Fe_1$  and  $Fe_2$  have respectively 4 and 1 sulfur atoms at distance less than 2.5 Å, and 6 and 11 iron atoms within the same distance.

FIG. 8. Iron and sulfur time dependent diffusion coefficients calculated using Eq. (4). The four panels refer to four different time windows taken to make the time averages (see text).

## REFERENCES

- [1] F. Birch, *J. Geophys. Res.*, **57**, 227 (1952).
- [2] S. P. Clark, *The Earth Sciences*, edited by T. W. Donnelly, University of Chicago Press, Chicago, (1963).
- [3] H.C. Urey, *Geochim. Cosmochim. Acta*, **18**, 151 (1960).
- [4] G. J. F. MacDonald and L. Knopoff, *J. Geophys.*, **1**, 1751 (1958).
- [5] A. E. Ringwood, *Geochim. Cosmochim. Acta*, **15**, 257 (1959).
- [6] A. E. Ringwood, *Geochim. Cosmochim. Acta*, **25**, 1 (1961).
- [7] A. E. Ringwood, *Geochim. Cosmochim. Acta*, **30**, 41 (1966).
- [8] B. J. Alder, *J. Geophys. Res.*, **71**, 4973 (1966).
- [9] F. Birch, *J. Geophys. Res.*, **69**, 4377 (1964).
- [10] B. Mason, *Nature*, **211**, 616 (1966).
- [11] V. Murthy and H.T. Hall, *Phys. Earth Planet. Inter.*, **2**, 276 (1970).
- [12] J. S. Lewis, *Annu. Rev. Phys. Chem.*, **24**, 339 (1973).
- [13] A. E. Ringwood, *Geochem. J.*, **11**, 111 (1977).
- [14] Y. Fukai and S. Akimoto, *Proc. Jpn. Acad., Ser. B*, **59**, 158 (1983).
- [15] T. Suzuki, S. Akimoto and T. Yagi, *Phys. Earth Planet. Inter.*, **56**, 377 (1989).
- [16] T. J. Usselman, *Am. J. Sci.*, **275**, 278 (1975).
- [17] T. J. Usselman, *Am. J. Sci.*, **275**, 291 (1975).
- [18] R. Brett and P. M. Bell, *Earth Planet. Sci. Lett.*, **6**, 479 (1969).
- [19] I. Štich, R. Car and M. Parrinello, *Phys. Rev. Lett.*, **63**, 2240 (1989).
- [20] G. Kresse and J. Hafner, *Phys. Rev. B*, **48**, 13115 (1993).
- [21] G. Kresse and J. Hafner, *Phys. Rev. B*, **49**, 14251 (1994).
- [22] F. Kirchhoff, J. M. Holender and M. J. Gillan, *Phys. Rev. B*, **54**, 190 (1996).
- [23] F. Kirchhoff, G. Kresse and M. J. Gillan, *Phys. Rev. B*, *in press*.
- [24] L. Vočadlo, G. A. de Wijs, G. Kresse, M. J. Gillan and G. D. Price, *Faraday Discuss.*, **106**, 205 (1997).
- [25] G. A. de Wijs, G. Kresse, L. Vočadlo, D. Dobson, D. Alfè, M. J. Gillan, G. D. Price, *Nature*, *in press*.
- [26] T. J. Arhens, *J. Geophys. Res.*, **89**, 6041 (1984).
- [27] G. E. LeBlanc and R. A. Secco, *Geophys. Res. Lett.*, **23**, 213 (1996).
- [28] Y. Wang and J. Perdew, *Phys. Rev. B*, **44**, 13298 (1991).
- [29] D. Vanderbilt, *Phys. Rev. B*, **41**, 7892 (1990).
- [30] S. G. Louie, S. Froyen and M. L. Cohen, *Phys. Rev. B*, **26**, 1738 (1982).
- [31] R. Car and M. Parrinello, *Phys. Rev. Lett.*, **55**, 2471 (1985).
- [32] P. Pulay, *Chem. Phys. Lett.*, **73**, 393 (1980).
- [33] G. Kresse and J. Furthmüller, *Comput. Mater. Sci.*, **6**, 15 (1996).
- [34] G. Kresse and J. Furthmüller, *Phys. Rev. B*, **54**, 11169 (1996).
- [35] R. W. G. Wyckoff, *Crystal Structures*, Vol. 1, Second edition, Interscience Publishers, New York (1963).
- [36] H. E. King Jr. and C. T. Prewitt, *Acta Crystallogr. B*, **38**, 1877 (1982).
- [37] L. A. Taylor and H. K. Mao, *Science*, **170**, 850 (1970).
- [38] R. O. Pichulo, J. S. Weaver, T. Takahashi, *Meteoritics*, **11**, 351 (1976).
- [39] H. E. King Jr., D. Virgo, H. K. Mao, *Carnegie Inst. Washington Year Book*, **77**, 830 (1978).

- [40] H. K. Mao, G. Zou and P. M. Bell, *Carnegie Inst. Washington Year Book*, **80**, 267 (1981).
- [41] D. M. Sherman, *Earth Planet. Sci. Lett.*, **132**, 87 (1995).
- [42] H. K. Mao, Y. Wu, L. C. Chen and J. F. Shu, *J. Geophys. Res.*, **95**, 21737 (1990).
- [43] J. P. Poirier, *Introduction to the Physics of the Earth's Interior*, Cambridge University Press (1991).
- [44] L. Verlet, *Phys. Rev.*, **159**, 98 (1967).
- [45] S. Nosé, *Molec. Phys.*, **52**, 255 (1984); *J. Chem. Phys.*, **81**, 511 (1984).
- [46] F. D. Di Tolla and M. Ronchetti, *Phys. Rev. B*, **48**, 1726 (1993).
- [47] F.A. Cotton, G. Wilkinson, *Advanced Inorganic Chemistry*, Wiley, New York (1988).
- [48] J. Friedel, in *The Physics of Metals*, ed. J. Ziman, p. 494, Cambridge University Press (1969).
- [49] M. P. Allen, D. J. Tildesley, *Computer Simulation of Liquids*, Oxford Science Publications (1987).
- [50] J. P. Hansen, I. R. McDonald, *Theory of Simple Liquids*, second edition, Academic Press, London (1986).
- [51] A. Eichler, J. Hafner, J. Furthmüller, G. Kresse, *Surf. Sci.*, **346**, 300 (1996).



FIGURE 1

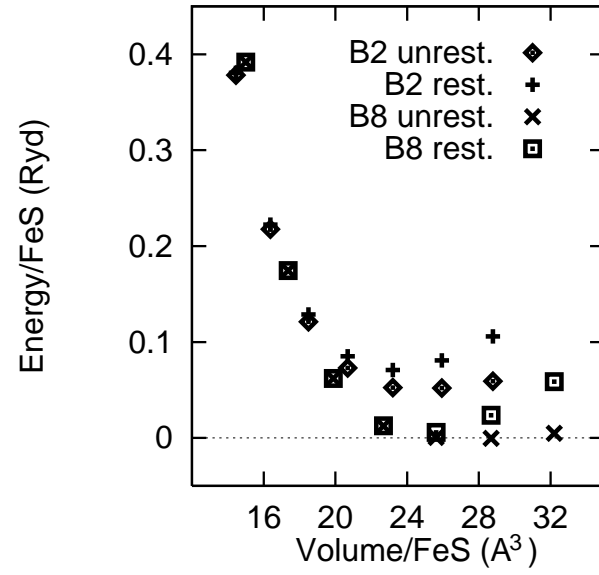


FIGURE 2

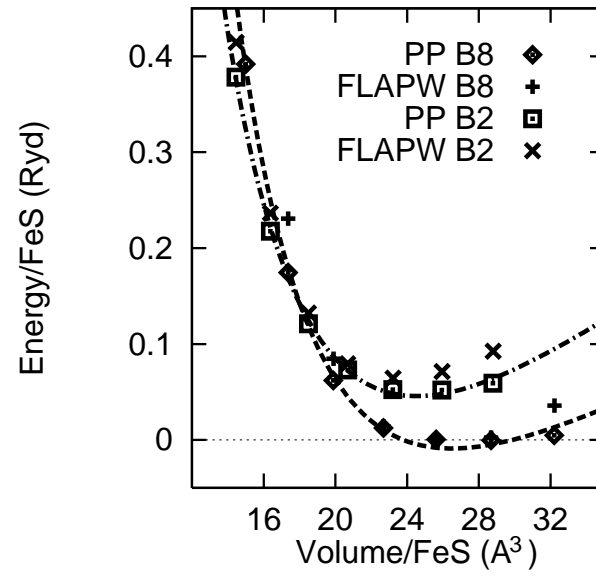


FIGURE 3

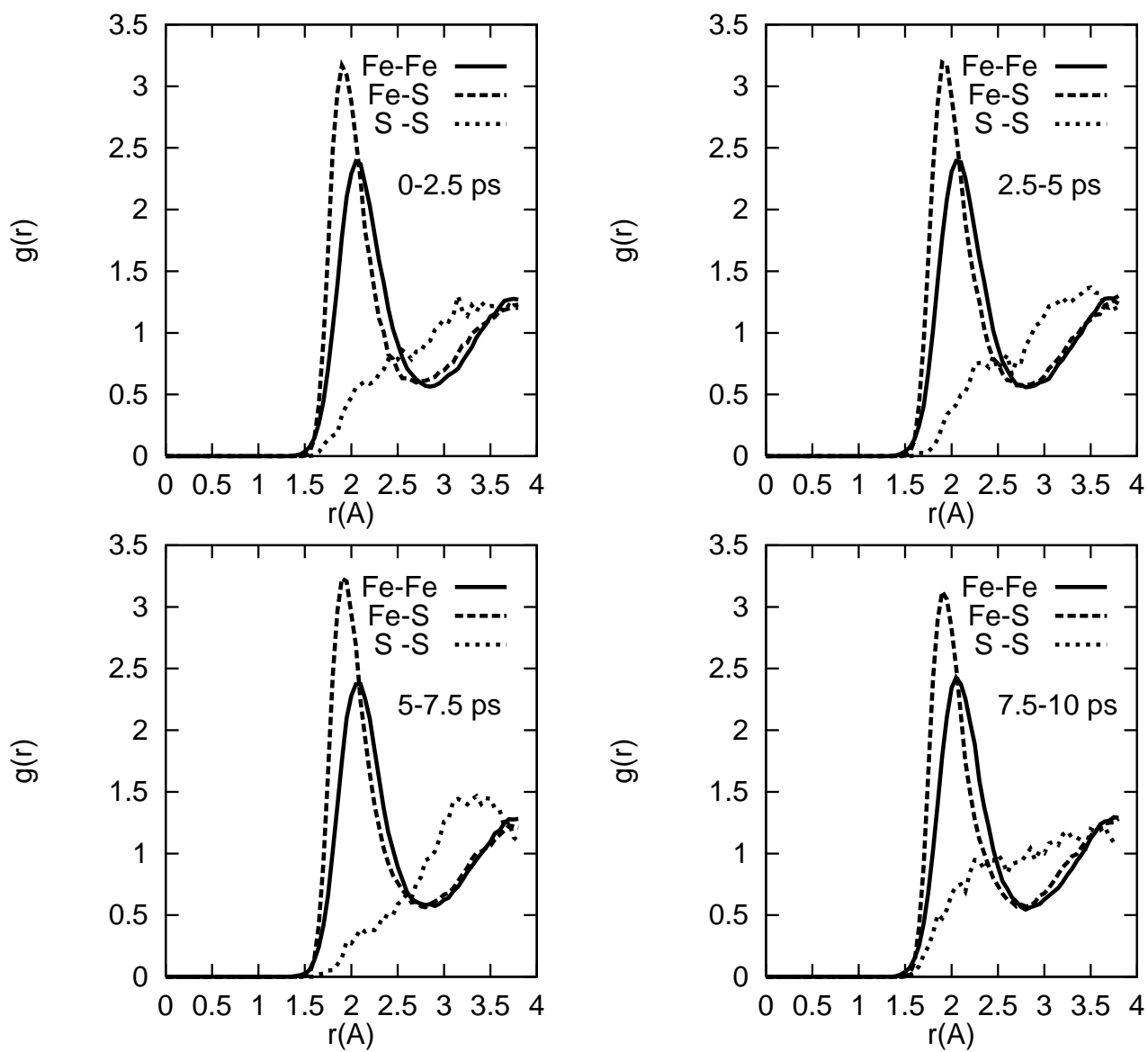


FIGURE 4

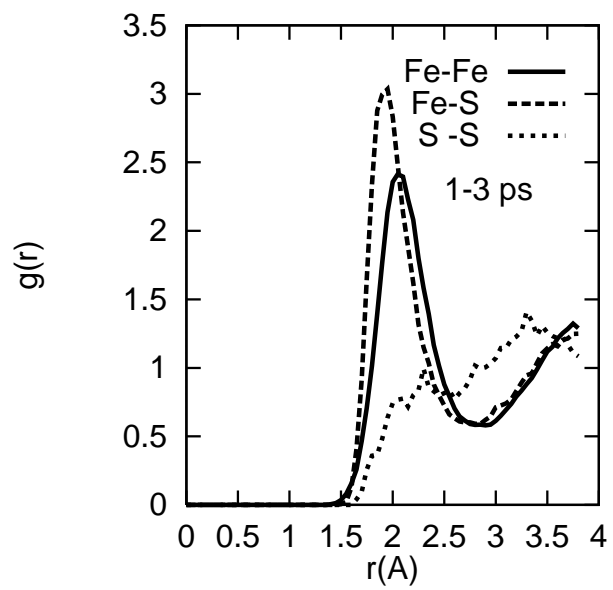
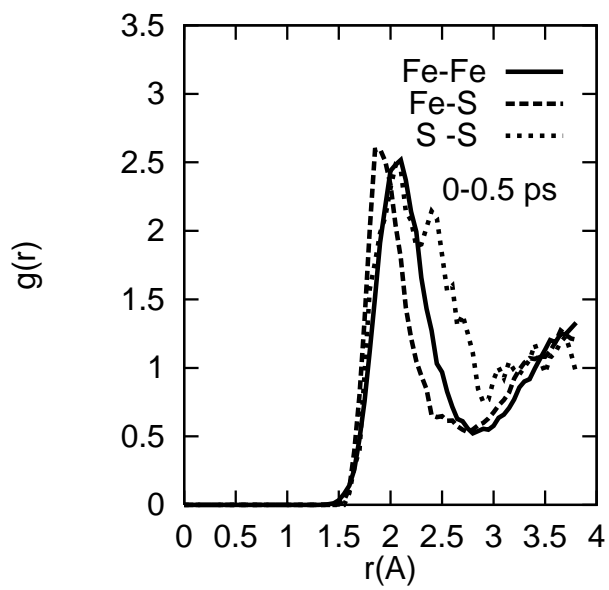


FIGURE 5

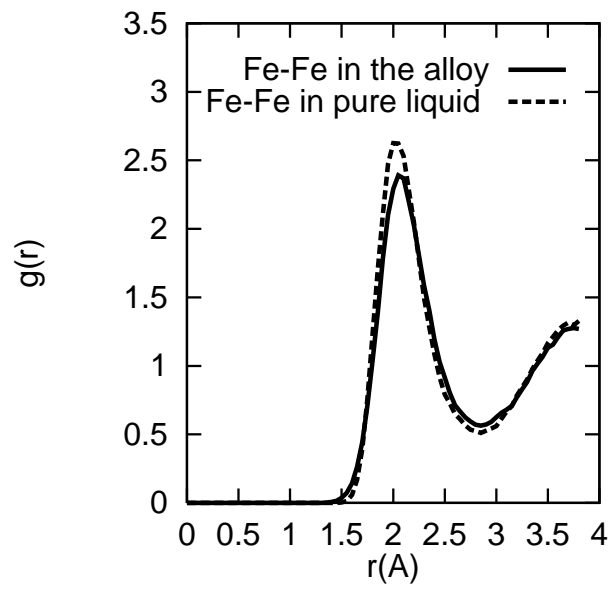


FIGURE 6

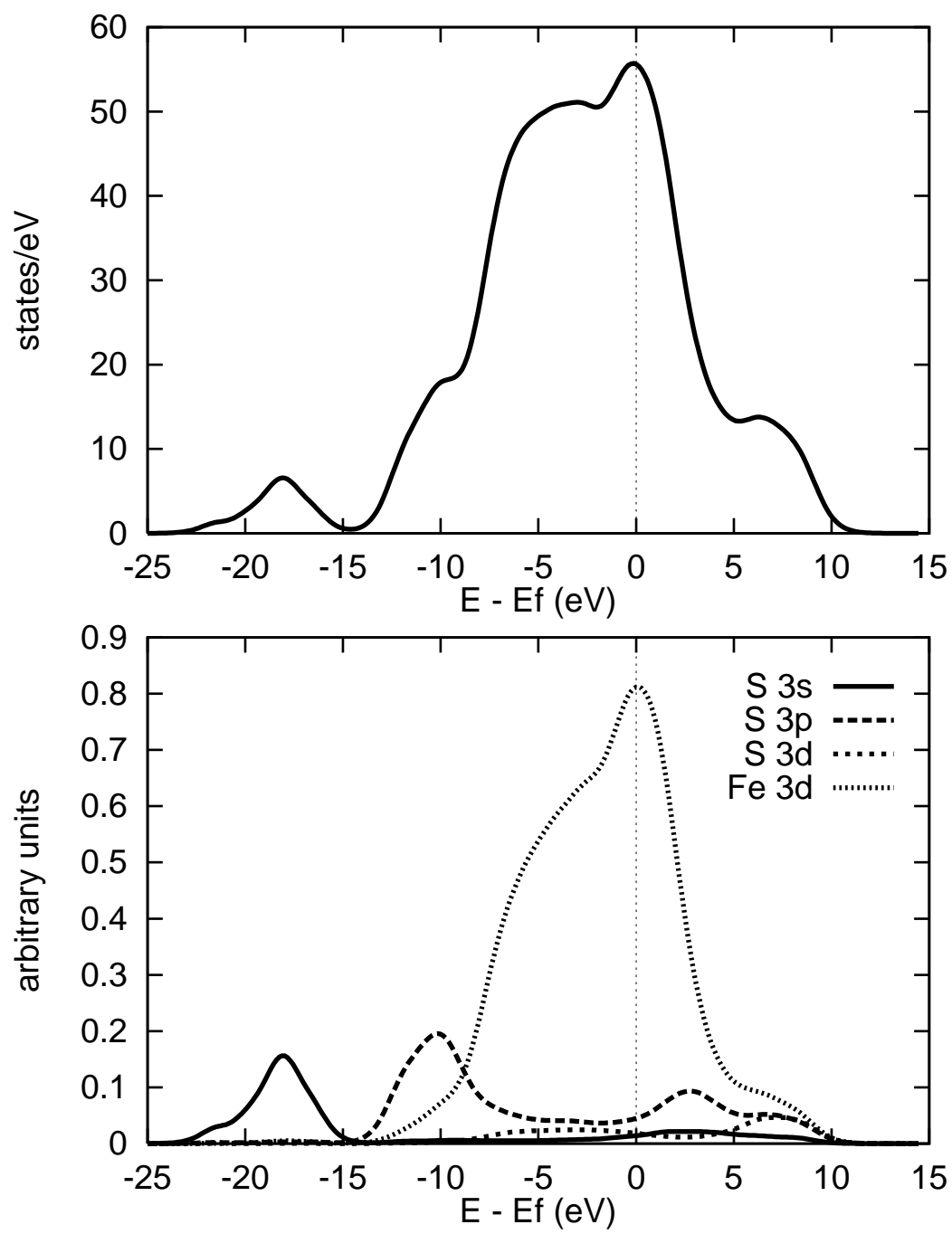


FIGURE 7

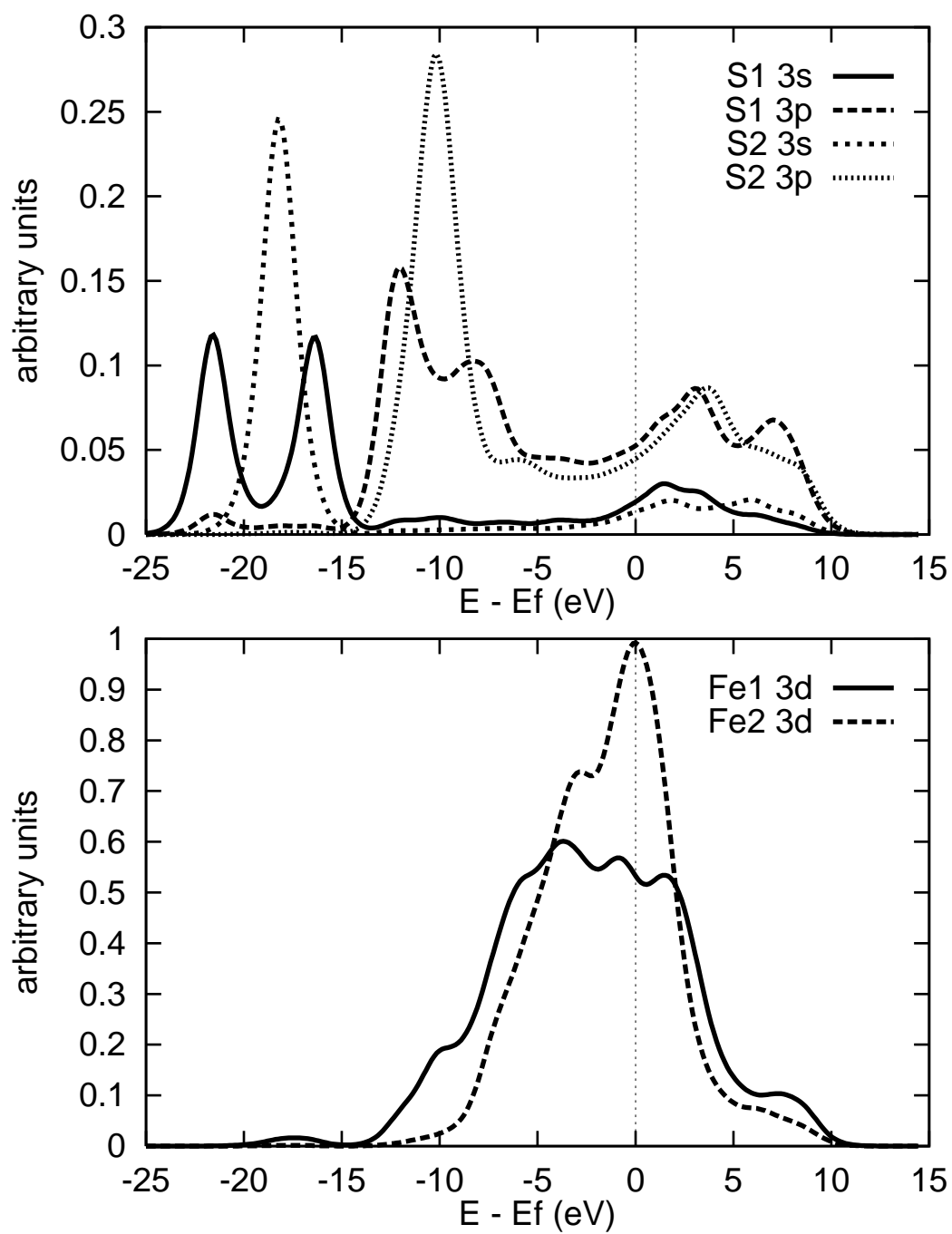


FIGURE 8

